Ultrafast (370 GHz bandwidth) *p-i-n* traveling wave photodetector using low-temperature-grown GaAs

Yi-Jen Chiu, Siegfried B. Fleischer, Daniel Lasaosa, and John E. Bowers
Department of Electrical and Computer Engineering, University of California at Santa Barbara, Santa Barbara, California 93106-9560

(Received 17 July 1997; accepted for publication 22 August 1997)

The authors demonstrate *p-i-n* traveling wave photodetectors utilizing low-temperature-grown GaAs as the absorption layer. The electro-optically measured impulse response was found to exhibit a pulsewidth of 1.1 ps full width at half maximum, corresponding to a −3 dB bandwidth of 370 GHz with an external quantum efficiency of 8% at 800 nm. © *1997 American Institute of Physics.* [S0003-6951(97)00243-X]

High speed and high-efficiency photodetectors are very important for microwave fiber-optical links. In the past few years, there has been considerable interest and progress in the fabrication of such detectors.[1–7] Vertical *p-i-n* photodetectors have been demonstrated to achieve high speed,[5] but to obtain a high bandwidth the carrier transit time must be short.[8] This requires a thin active region causing a low efficiency (limited bandwidth efficiency product: ∼30 GHz).[5] Surface-illuminated MSM photodetectors based on low-temperature-grown GaAs (LTG-GaAs)[1–3] achieve high speed performance because of the short carrier lifetime in LTG-GaAs. The bandwidth of these MSMs is carrier-recombination-time limited instead of carrier-transit-time limited. Although the speed is enhanced by the LTG-GaAs material, the improved bandwidth is again obtained at the expense of a low quantum efficiency. The edge-coupled traveling wave photodetector (TWPD) overcomes this limitation and thus improves the bandwidth-efficiency product. By distributing the RC elements and impedance matching to external circuits, both *p-i-n* and MSM-types of TWPD[4,6] show high bandwidth-efficiency products. In this work, we demonstrate a high speed *p-i-n* TWPD incorporating a LTG-GaAs active layer. The device performance was found to be enhanced by taking advantage of both the short carrier lifetime of the LTG-GaAs and the TWPD structure. The photodetectors were successfully fabricated and an impulse response of 1.1 ps full width at half maximum (FWHM) was measured using electro-optical sampling.

The structure for this photodetector was grown in a Varian GEN II solid source molecular beam epitaxy (MBE) system on a (100) semi-insulating GaAs substrate. The substrate temperature was set to 630 °C for about 5 min to desorb surface oxide under an As_2 overpressure of 9×10^{-6} Torr. The wafer was then cooled down to 570 °C for the onset of the layer deposition. Figure 1 (circular inset) shows a schematic plot of the *p-i-n* epitaxial layers. A 3 μm $Al_{0.5}Ga_{0.5}As$ layer was deposited just below the *p-i-n* waveguide to serve as the cladding layer to isolate the optical guided mode from the GaAs substrate. The *p-i-n* structure is optimized for both optical mode guiding and also for its electrical characteristics as the active region of the photodetector. The *n*- and *p*-type cladding layers ($Al_{0.2}Ga_{0.8}As$) of the waveguide were doped with Si and Be, respectively, and were grown under conditions identical to those in Ref. 6. In contrast to the detectors studied in Ref. 6 we utilized a LTG-GaAs layer as the optical absorption layer (*i* layer, 170 nm) instead of normal GaAs, thus allowing a good evaluation of effect of the LTG-GaAs on the device performance. The LTG-GaAs film was deposited at 215 °C (measured with a thermocouple temperature sensor) and then *in situ* annealed at 590 °C for 10 min. We found these growth conditions to be optimum for a short carrier lifetime and a good surface morphology (pump-probe measurements show a 350 fs decay time). The *n*-doped $Al_{0.2}Ga_{0.8}As$ and GaAs layers deposited on top of the LTG-GaAs active region were grown at a temperature of 570 °C.

A cross section drawing of TWPD is schematically shown in Fig. 1 (top). Figure 2 (top) shows the top view of the whole device. The total device was fabricated in eight steps. The metal region for the *n* contact was formed by standard lithography. Ni/AuGe/Ni/Au metal evaporation (e

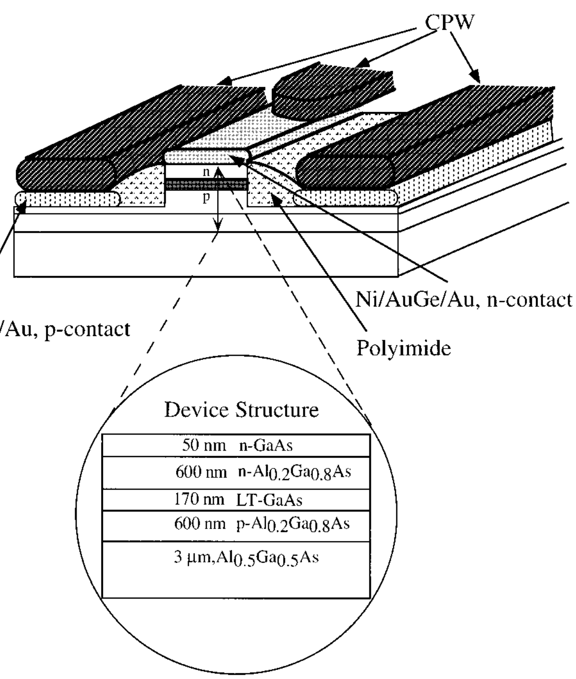

FIG. 1. Schematic cross section of the *p-i-n* region. The circular inset shows the details of the layer structure. The two ground lines of CPW were on top of *p* contacts and extended to the outside of the *p-i-n* region. The signal line of CPW was connected at the end of *n* contact. All etching surfaces were passivated by polyimide.

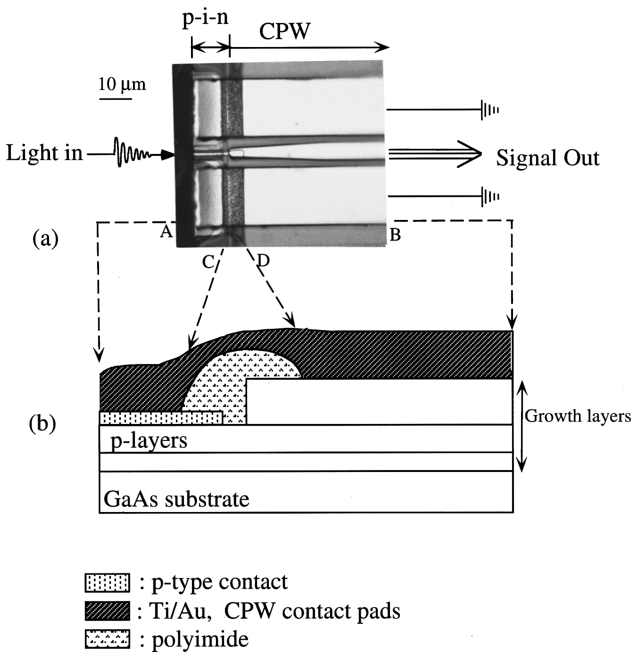

FIG. 2. (a) Top view of the low-temperature-grown (LTG) GaAs traveling-wave photodetector (TWPD). The light is edge coupled and the electrical signal from the *p-i-n* region is coupled to the coplanar waveguide (CPW). (b) The schematic plot of cross section ''A-B.'' The region of ''C-D'' was the polyimide area. The polyimide is used to bridge two ground lines from *p* contact of the *p-i-n* region to the CPW region.

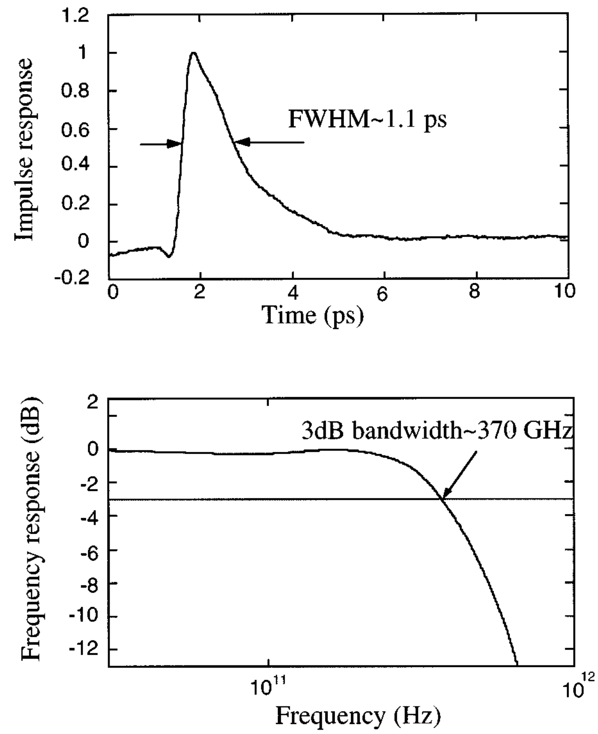

FIG. 3. Measured response of the low-temperature-grown (LTG) GaAs traveling-wave photodetector (TWPD). The top plot is the electro-optically-detected impulse response, which shows a 1.1 ps FWHM. The bottom is the corresponding Fourier transform (power spectrum).

beam) was used for the *n*-type contact (top portion of the *p-i-n*). This metal layer served as the mask for the subsequent Cl_2 reactive ion etching (RIE). As shown in Fig. 1 (top) and Fig. 2 (bottom), the RIE etch proceeded through the *n* layers, through the *i* layer (LTG-GaAs), and approximately 100 nm into the *p*-AlGaAs layer. Then, following similar processing steps, the *p*-type contact (Cr/AuZn/Au) was patterned on the p-$Al_{0.2}Ga_{0.8}As$ layer by thermal evaporation. Both the *p*- and *n*-type regions were then rapid-thermal annealed (RTA) at 380 °C for 30 s. After finishing the *p-i-n* regions, H^+ ion implantation was used to render the remaining areas (the right part of Fig. 2) semi-insulating, such that the microwave coplanar-waveguide (CPW) lines can be put on the top. A polyimide layer was spun on for passivation of the etching surface and for bridging the interconnection between *p-i-n* and the ground lines of CPW, which is schematically shown in Fig. 2 (bottom). Finally, Ti/Au was used for the metallization of CPW.

The devices were first characterized with a 50 GHz sampling scope using a 100 μm pitch coplanar microwave probe (40 GHz bandwidth). The obtained response was found to be instrument limited. A back bias of 3 V was applied for all our measurements. To determine the actual speed of the TWPD electro-optic (EO) sampling was used for further characterization. The optical excitation pulses for the EO-sampling measurements were obtained from a mode locked Ti:sapphire laser operating at a wavelength of 800 nm[9] and with a 100 fs optical pulse width. An optical pulse energy of 0.3 pJ (not accounting for coupling or reflection losses) was used for the optical excitation. The laser was edge coupled into the optical waveguide surrounding the *p-i-n* region of the detector. After absorption of the optical pulse and generating the electrical signal in the TWPD, the microwave impulses were propagated along the CPW lines. On the CPW, the EO pump-probe signal was detected utilizing the electro-optic effect in a $LiTaO_3$ crystal placed on the CPW structure.[10]

At high frequencies dispersive effects of the transmission line may be considerable and can affect the time signature of the measured picosecond detector response. A CPW ($\sim 5\ \mu$m electrode separation) on a substrate with a microwave dielectric constant of $\epsilon_{rel} \sim 43$ for $LiTaO_3$ and $\epsilon_{rel} \sim 13.2$ for GaAs has estimated critical frequencies of 2.5 and 5 THz, respectively.[11] Above the critical frequency, modal dispersive effects due to higher order modes become significant. The measured signals we obtained are, however, much slower than these critical frequencies and modal dispersive effects can thus be neglected. To further minimize pulse broadening due to modal and waveguide dispersion, our EO sampling data were taken as close to the photodetector as possible ($\sim 50\ \mu$m distance).

The electro-optically determined impulse responses are shown in Fig. 3. The optical power level was kept low to avoid carrier saturation and barrier blocking effects, i.e., the device was operated in the linear region. The measured FWHM value is around 1.1 ps. The device has overcome the carrier transit time limit which limited previous results.[6] The Fourier transform power spectrum of the measured signal shows a 3 dB bandwidth of 370 GHz.

Reflections from the boundaries of EO crystal may interfere with the original pulse from the photodetector. To verify that our measurements were not affected by such reflections, we took EO-sampling data at various positions along the CPW lines. None of our data showed any echoes corresponding to reflections of the interfaces of the $\sim$500-μm-long $LiTaO_3$ crystal. Even though the $LiTaO_3$ has a higher dielectric constant than GaAs, the EO crystal is only resting on the GaAs and an air gap of several microns between the crystal and the GaAs is to be expected. Such a gap will decouple the waveguide mode from the crystal because of the small electrode separation of only 5 μm used for our samples.

A dc efficiency measurement revealed an external quantum efficiency of 8%. The efficiency was obtained at a reverse bias voltage of 3 V using free space lens coupling without antireflection (AR) coating. Theoretically, we expect an internal quantum efficiency of 20%. This estimate assumes a carrier lifetime of 350 fs[12] and neglects intrinsic losses in the optical waveguide. After accounting for the reflection losses and the imperfect mode matching, the measured efficiency agrees with the theoretically predicted value.

In summary, we have demonstrated a novel traveling wave photodetector grown by LTG-GaAs. The photodetector impulse response has a FWHM of only 1.1 ps and a -3 dB bandwidth of 370 GHz. To our knowledge this is the highest bandwidth reported for a *p-i-n* photodetector. The photodetector is limited by the carrier recombination rate rather than the carrier transit time. The external quantum efficiency is better than 8%, similar to other photodetectors fabricated with LTG-GaAs layers. A sub-picosecond response and quantum efficiencies of better than 20% should be possible.

The authors thank M. J. W. Rodwell for valuable discussions and S. Z. Zhang, Y. H. Jan, T. Reynolds, and Kirk S. Giboney for help with the mask, process, and measurements. This work is supported by the Center for Nonstoichiometric III–V Semiconductors under program No. F49620-95-1-0394 (AFOSR, Dr. G. Witt).

[1] S. Y. Chou and M. Y. Liu, IEEE J. Quantum Electron. **28**, 2358 (1992).
[2] E. R. Brown, K. A. McIntosh, K. B. Nichols, and C. L. Dennis, Appl. Phys. Lett. **66**, 285 (1991).
[3] Y. Chen, S. Williamson, and Tim Brock, Appl. Phys. Lett. **59**, 1984 (1991).
[4] L. Y. Lin, M. C. Wu, T. Itoh, T. A. Vang, R. E. Muller, D. L. Sivco, and A. Y. Cho, IEEE Photonics Technol. Lett. **8**, 1376 (1996).
[5] Y. G. Wey, K. S. Giboney, J. E. Bowers, M. J. Rodwell, P. Silvestre, P. Thiagarajan, and G. Y. Robinson, IEEE Photonics Technol. Lett. **7**, 412 (1993).
[6] K. S. Giboney, R. L. Nagarajan, T. E. Reynold, S. T. Allen, R. P. Mirin, M. J. W. Rodwell, and J. E. Bowers, IEEE Photonics Technol. Lett. **7**, 412 (1995).
[7] I.-H. Tan, C.-K. Sun, K. S. Giboney, J. E. Bowers, E. L. Hu, B. I. Miller, and R. J. Capik, IEEE Photonics Technol. Lett. **7**, 1477 (1995).
[8] S. M. Sze, *Physics of Semiconductor Devices*, 2nd ed. Chap. 13.
[9] E. S. Harmon, D. T. McInturff, M. R. Melloch, and J. M. Woodall, J. Vac. Sci. Technol. B **13**, 768 (1995).
[10] T. Itatani, T. Nakagawa, F. Kano, K. Ohta, and Y. Sugiyama, IEICE Trans Electron. **1**, 73 (1995).
[11] J. A. Valdmanis and G. Mourou, IEEE J. Quantum Electron. **22**, 69 (1986).
[12] E. R. Brown, K. A. McIntosh, K. B. Nichols, M. J. Manfra, and C. L. Dennis, Proc. SPIE **2145**, 200 (1994).